RESEARCH ARTICLE

Spatial distribution and risk assessment of heavy metals inside and outside a typical lead-zinc mine in southeastern China

Xuchao Zhu[1] · Longxi Cao[2] · Yin Liang[1]

Abstract

Mining activity is an important source of heavy metals in soil. Understanding the contents and distribution of heavy metals in mineral-waste soil and surrounding environments is important for the rational management of mines and reducing the migration of heavy metals to surrounding environments. We used a non-ferrous metal mine in southern China as a research object. Three types of sampling site (A–C) were established on the mineral-waste soil in the mining area and on nearby farmland (D) and along a river channel (E) outside the mining area: A, newly processed mineral-waste soil; B, steep 6-month-old stack of waste soil; C, gentle slope of 12-month-old waste soil; D, farmland soil within 1 km of the mine; and E, river water and adjacent soil. Soil samples were collected from the 0–10-cm layer at each site type. The contents and spatial distribution of Pb, Zn, and Cd at the sampling sites were analyzed, and the environmental risks were evaluated. The mean Pb, Zn, and Cd contents in the mining area (types A–C) were 2028, 3794, and 14.8 mg kg^{-1}, respectively, which were 8-, 19-, and 49-fold higher than the second-level limits of the Environmental Quality Standard for Soils of China, and the mean contents of Pb, Zn, and Cd for sites D and E were 76.4, 131, and 0.18 mg kg^{-1} and 147, 194, and 0.95 mg kg^{-1}, respectively, all of which were under the second-level limits. Sites C and E were also used to analyze the spatial distribution of the Pb, Zn, and Cd contents. Geostatistical analysis found that the Pb, Zn, and Cd contents had a clear and similar spatial pattern at site C and generally decreased from north to south. Soil Pb, Zn, and Cd contents at site E generally increased, and water Pb, Zn, and Cd concentrations decreased along the river channel. The soils at site types A–C in the mining area were heavily polluted, with a high potential threat to the surrounding environment, and the farmland and river-bank soils at D and E were free of pollution or were lightly polluted, with low potential ecological risks. This study provides a scientific basis and supporting data for heavy-metal treatment in mining areas.

Keywords Heavy metal · Mineral-waste soil · Spatial distribution · Risk assessment · Sampling site type

Introduction

Heavy metals in soil have received great attention worldwide due to the development of industry, mining, and urbanization (Chen et al. 2009; Rodrigues et al. 2006). Heavy metals are

difficult to degrade in soil and will accumulate and then enter the food chain, which seriously threatens human health (Ding et al. 2017). The heavy metals in soil have two sources: natural and anthropogenic. The natural sources are mainly from geo-chemical processes associated with the soil parental material. The anthropogenic sources are mainly from mining and agri-cultural activities and the combustion of fossil fuels, which release much more heavy metals than the natural sources (Liang et al. 2017; Marrugo-Negrete et al. 2017). Mineral mining and smelting produce a large amount of waste soil enriched in heavy metals, which poses strong threats to the surrounding environment due to surface runoff and soil ero-sion (Duan et al. 2015).

Traditional studies of pollution by heavy metals caused by mining activities have mainly focused on soil outside the min-ing areas, including analyzing the content based on classical statistics and using relevant standards for determining the

---

✉ Yin Liang
  yliang@issas.ac.cn

[1] State Key Laboratory of Soil and Sustainable Agriculture, Institute of Soil Science, Chinese Academy of Sciences, No. 71 of Beijing East Road, Xuanwu District, Nanjing 210008, Jiangsu Province, China

[2] College of Earth Science, State Environmental Protection Key Laboratory of Synergetic Control and Joint Remediation for Soil & Water Pollution, Chengdu University of Technology, Chengdu 610059, China

pollution level (Liang et al. 2017), determining the spatial distribution of heavy metals using Kriging interpolation based on geostatistics (Alary and Demougeot-Renard 2010; Reza et al. 2015; Yan et al. 2015), assessing pollution levels and potential risks using indices such as the single-factor pollution index (P), Nemerow synthetic pollution index (P_N), potential ecological risk index (RI) and geoaccumulation index (I_{geo}) (Duan et al. 2015; Marrugo-Negrete et al. 2017), and using correlation, principal component, and cluster analyses to determine the source of heavy metals (Fu and Wei 2013; Liu et al. 2016; Ma et al. 2016). The effects of topography, soil, climate, and other factors on the spatial distribution of heavy metals in soils (Bednářová et al. 2016; Ding et al. 2017; Maas et al. 2010), effects of heavy-metal ions in mineral drainage on the soil environment (Li et al. 2009), and contents and distribution of heavy metals in the sediments of rivers, reservoirs, and lakes (Wang et al. 2012, 2014; Wang et al. 2015) have also been studied. Studies of the content and distribution of heavy metals in mineral-waste soils with different stacking times and their influence on the surrounding environment, including nearby farmland, river water, and bank soil, however, are rare. The heavy-metal content in waste soil varies with stacking time due to the influence of natural dispersal, including slope runoff, rainwater leaching and wind, and the potential hazards to the surrounding soil and aquatic environments also differ (Lu et al. 2017). Knowing the content, distribution, and influencing factors of heavy metals in mineral-waste soils will provide supporting data for effective treatment, control of the spread of pollution, protection of the surrounding soil and aquatic environments, and assurance of food quality and human health.

The objectives of this study were therefore to (1) determine the contents of typical heavy metals, i.e., lead (Pb), zinc (Zn), and cadmium (Cd) in the mineral-waste soil at a mine and in the soil in surrounding farmland and along a nearby river; (2) identify the spatial distributions of the three heavy metals within (in a gently sloping stack of waste soil) and outside (along the river) the mining area; and (3) assess the degree of pollution by the three heavy metals in the soils and river water and the potential threat to the environment at the five site types.

Materials and methods

Study area

The mining area we used as a research object is in northeastern Jiangxi Province, China (Fig. 1a; 27°54′N, 117°11′E) and has a subtropical humid monsoon climate. The average annual air temperature in the area from 1953 to 2016 was 18.5 °C based on meteorological data from the Guixi meteorological station (28°11′N, 117°09′E). The average temperatures in the hottest

and coldest months were 30.0 °C (July) and 6.2 °C (January), respectively, and the average annual rainfall was 1891 mm, 2/3 of which fell from March to July. The area is dominated by low mountains and hills, and rivers and valleys are common (Fig. 1b). The mine of non-ferrous metals was at the foot of the mountains. Mineral-waste soil has been stacked between the two mountains and has formed a large stack about 200 m long and wide and several tens of meters deep. Rainwater falls on the stack, the water flows into a sewage-treatment plant through artificial ditches on one slope and is then discharged into a nearby river after treatment. On the other slope, runoff is produced and converges naturally, flowing through the surface of waste soils with different stacking times (Fig. 1c) and then flowing into a sedimentation tank. The mine is a typical source of Pb and Zn ore, where the contents of Pb and Zn are higher than other heavy metals, and Cd is an extensively studied heavy metal in the field of food safety, so we chose Pb, Zn, and Cd as the objects of this study.

Experimental design and data acquisition

We studied five types of sampling sites. Three types (A–C) were stacks of mineral-waste soil in the mining area, and two types (D and E) were farmland and a river channel outside of the mining area. Soil samples were collected using an auger to a depth of 10 cm and were wrapped in ziplock bags. Water samples were collected from the nearby river using 500-ml plastic bottles. Site type A was an area with new mineral-waste soil that had fallen from a mine conveyor belt. Three bags of samples of about 300 g each were collected for analyzing Pb, Zn, and Cd contents in the original waste soil. Type B was a steep slope on a stack of mineral-waste soil with a stacking time of about 6 months (Fig. 1c). Six samples were collected in the upper, middle, and lower positions of the slope after 6 months of erosion and leaching. Type C was a gentle slope of about 15×20 m with a stacking time of about 12 months. Samples were collected at 36 points in a 2×4 m grid (Fig. 1d) for analyzing the content, spatial variation, and distribution of the three heavy metals after erosion and leaching for 12 months. Type D consisted of three farms within 1 km around the mining area (Fig. 1b). One composite soil sample was collected at each farm for analyzing the heavy-metal contents and potential hazards. Type E was along the nearby river, with the point where the treated runoff was discharged as the origin (E0). Soil and water samples were collected 2 km upstream (E-1 and E-2) and 8 km downstream (E1, E2,…, E8) at intervals of 1 km, for a total of 11 soil samples and 11 water samples, for analyzing the spatial distribution and environmental risk of heavy metals in the river water and riverside soil. The characteristics of types A-E are summarized in Table 1.

The soil samples were naturally air-dried in a ventilated room after gravel, plant roots, and other debris had been removed. The samples were then ground and passed through a 100-mesh nylon sieve. The samples were weighed to 0.25 g
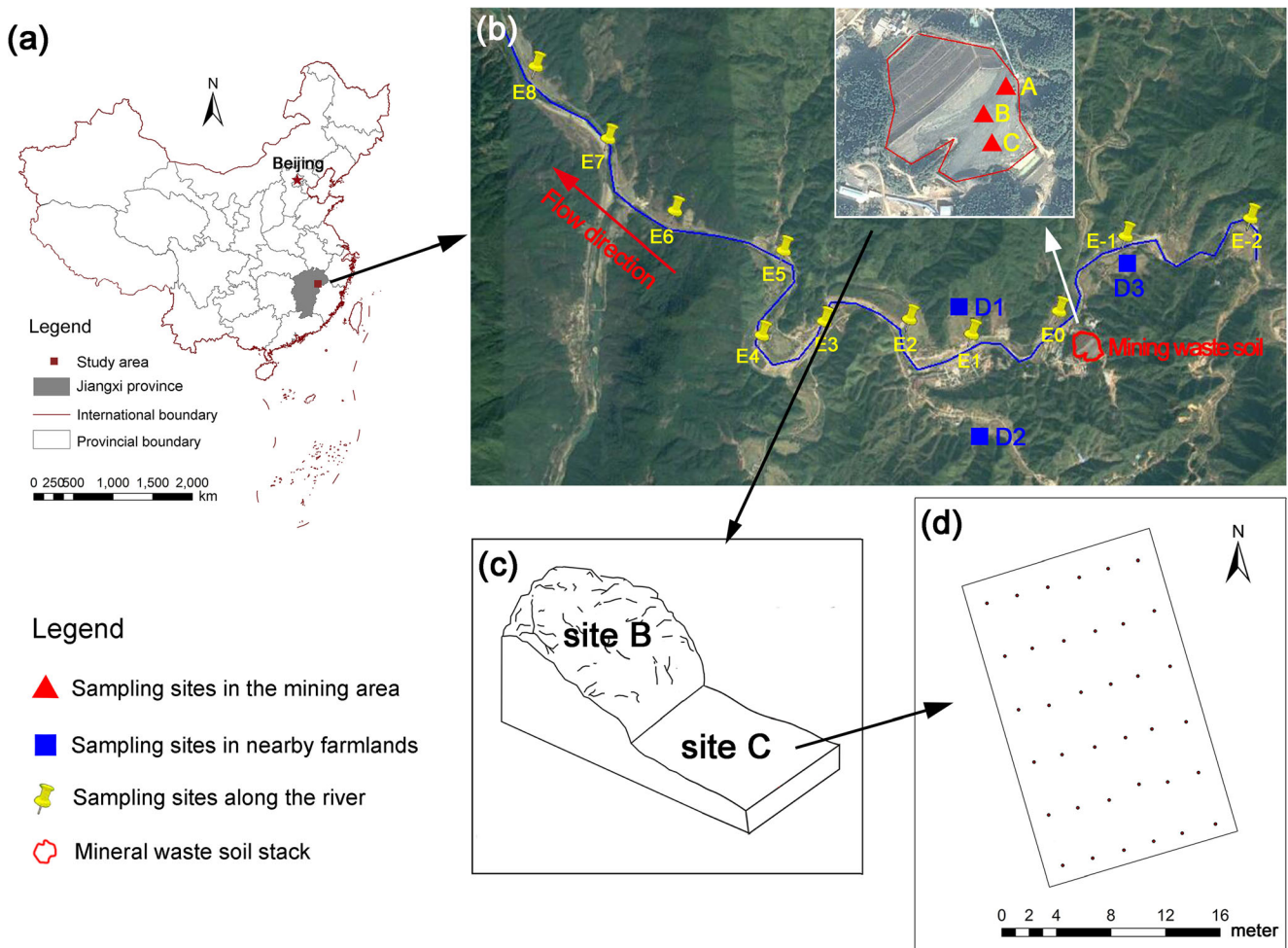
Fig. 1 Location of the study area in China (**a**), the five types of sampling sites (**b**), schematic diagram of the steep 6-month-old stack of waste soil (site B) and gentle slope of 12-month-old waste soil (site C) of waste soil (**c**) and sampling design on the gentle slope (**d**)

and then dissolved using nitric, perchloric, and hydrofluoric acids. High-performance liquid chromatography (HPLC 1100, Agilent, USA) and inductively coupled plasma mass spectrometry (Optima 8000, PerkinElmer, USA) were used for measuring the Pb, Zn, and Cd contents.

The latitude, longitude, and elevation of each point in site type C were measured using differential GPS. A digital elevation model was interpolated in ArcGIS based on the elevations and was then used to extract a terrain index for slope and aspect and slope hydrological indices for water-flow direction (FD) and flow accumulation (FA) in the hydrological analysis module, which were used to determine the influence of these parameters on the heavy metal contents.

Table 1 Summary of the five types of sampling sites

Location	Site type	Description	Sample type	Sample number
Inside the mining area	A	new mineral waste	mineral waste soil	3
	B	mineral waste stacked for about 6 months; steep slope	mineral waste soil	6
	C	mineral waste stacked for about 12 months; gentle slope	mineral waste soil	36
Outside the mining area	D	three directions within 1 km of the stacks of mineral waste	farmland soil	3
	E	2 km upstream and 8 km downstream from the discharge point at intervals of 1 km	river soil and water	11 + 11

Table 2 Descriptive statistics of Pb, Zn, and Cd contents (mg kg^{-1}) in site types A, B, C, and D

Site type	Heavy metal	Minimum	Mean	Maximum	SD[a]	CV[b] (%)
A	Pb	2799	2856	2918	59.6	2.1
	Zn	5198	5686	5986	427	7.5
	Cd	23.9	25.4	26.6	1.4	5.5
B	Pb	1676	1989	2277	213	10.7
	Zn	2861	3162	3361	177	5.6
	Cd	13.3	16.1	19.1	2.1	12.8
C	Pb	1305	1966	2995	378	19.2
	Zn	2899	3742	4878	524	14.0
	Cd	9.4	13.7	18.2	2.0	14.8
D	Pb	56.8	76.4	96.8	20.0	26.2
	Zn	103	131	151	24.8	19.0
	Cd	0.07	0.18	0.27	0.10	56.0

[a] Standard deviation

[b] Coefficient of variation

Methods of risk assessment

Excessive levels of Pb, Zn, and Cd in the soil and river water were determined based on the second-level limits of the Environmental Quality Standard for Soils of China (1995) and Surface Water Environmental Quality Standard of China (2002), respectively. The second-level limits for Pb, Zn, and Cd contents in the soil are 250, 200, and 0.3 mg kg^{-1}, respectively, which are used to ensure the security of agricultural production and to protect human health. The limits for Pb, Zn, and Cd concentrations in surface water are 10, 1000, and 5 μg L^{-1}, respectively, and are used to ensure the security of centralized domestic drinking water.

We used four pollution indices, single factor pollution index (P), Nemerow synthetic pollution index (P_N), potential ecological risk index (RI), and geoaccumulation index (I_{geo}), to assess the degree of pollution and potential environmental risk. The degree of pollution by each heavy metal can be determined directly and simply using P:

$$P_i = \frac{C_i}{S_i} \tag{1}$$

where P_i is the pollution index of heavy metal i, C_i is the measured content of heavy metal i (mg kg^{-1}), and S_i is the standard value of heavy metal i. The second-level limits of the Environmental Quality Standard for Soils of China (1995) were used here, with standard values for Pb, Zn, and Cd of 250, 200, and 0.3 mg kg^{-1}, respectively.

P_N represents the comprehensive impact of multiple heavy metals and highlights the environmental hazards of the most polluting metal:

$$P_N = \sqrt{\frac{P_{i,ave}^2 + P_{i,max}^2}{2}} \tag{2}$$

where $P_{i,ave}$ and $P_{i,max}$ are the mean and maximum values of the pollution index for heavy metal i, respectively. $P_N \leq 0.7$ indicates no pollution, $0.7 < P_N \leq 1$ indicates borderline pollution, $1 < P_N \leq 2$ indicates low-level pollution, $2 < P_N \leq 3$ indicates moderate pollution, and $P_N > 3$ indicates high-level pollution.

RI represents the degree of the potential environmental risk from heavy metals and is a comprehensive index that considers the toxicity, ecological effect, and environmental effect (Hakanson 1980):

$$RI = \sum_{i=1}^{n} (T_i \times P_i) \tag{3}$$

where n is the number of heavy metals and T_i is the toxicity coefficient of heavy metal i. T_{Pd}, T_{Zn}, and T_{Cd} were 5, 1, and 30, respectively, according to the study of Hakanson (1980). The potential risk is generally considered to be low at $RI < 150$, moderate at $150 \leq RI < 300$, considerable at $300 \leq RI < 600$, and high at $RI \geq 600$.

I_{geo} is an index that represents the influence of natural geological processes and human activity on heavy-metal pollution (Wang et al. 2014):

$$I_{geo} = \log_2 \frac{C_i}{1.5 \cdot B_i} \tag{6}$$

where B_i is the background value of heavy metal i in the study area; B_{Pb}, B_{Zn}, and B_{Cd} are 32.3, 69.4, and 0.108 mg kg^{-1}, respectively, in this study area according to the background values of soil elements of China (National Environmental Monitoring Centre of China 1990), and 1.5 is a correction factor associated with rock geology and sedimentary characteristics. I_{geo} consists of seven classes: $I_{geo} \leq 0$, uncontaminated; $0 < I_{geo} < 1$, from uncontaminated to moderately contaminated; $1 < I_{geo} < 2$, moderately contaminated; $2 < I_{geo} < 3$,

from moderately to strongly contaminated; $3 < I_{geo} < 4$, strongly contaminated; $4 < I_{geo} < 5$, from strongly to extremely contaminated; and $I_{geo} > 5$, extremely contaminated (Marrugo-Negrete et al. 2017).

Statistics and analysis

We analyzed the data using classical statistics and geostatistics. The classical descriptive statistical parameters minimum, mean, maximum, standard deviation (SD), coefficient of variation (CV, the ratio of SD to the mean), kurtosis, and skewness were calculated to determine the magnitude, variability, and normality of the variables. The variation of a variable was determined using CV. The variability of a variable was weak, moderate, and strong when $CV \leq 10\%$, $10\% < CV < 100\%$, and $CV \geq 100\%$, respectively, based on the classification standard of Nielsen and Bouma (1985).

Geostatistics was used to describe the spatial structure of the variation of the variables. The most important step was to calculate the semivariance of the variables:

$$\gamma(h) = \frac{1}{2N(h)} \sum_{i=1}^{N(h)} [Z(x_i) - Z(x_i + h)]^2 \qquad (7)$$

where $\gamma(h)$ is the semivariance, h is the spatial distance between two sampling points, $Z(x_i)$ and $Z(x_i + h)$ are the values of a variable at points i and i + h, respectively, and $N(h)$ is the number of pairs of sample points separated by h. The semivariance values were used to build semivariance models and the models used in this study were spherical, linear, and exponential models. The equations were

$$\gamma(h) = \begin{cases} C_0 + C\left[\frac{2}{3}\left(\frac{h}{a}\right) - \frac{1}{2}\left(\frac{h}{a}\right)^2\right] & h \leq a \\ C_0 + C & h > a \end{cases} \qquad (8)$$

$$\gamma(h) = \begin{cases} C_0 + C\left(\frac{h}{a}\right) & h \leq a \\ C_0 + C & h > a \end{cases} \qquad (9)$$

$$\gamma(h) = C_0 + C\left[1 - \exp\left(-\frac{h}{a}\right)\right] \qquad (10)$$

where a is the range; C_0 is the nugget, which represents the variance caused by random error; C is the structural variance, which is caused by systemic factors; $C_0 + C$ is the sill, which represents the total variance of the variable; and $C_0/(C_0 + C)$ is the spatial heterogeneity ratio. A variable is weakly, moderately, and strongly spatially dependent when $C_0/(C_0 + C) \geq 75\%$, $25\% < C_0/(C_0 + C) < 75\%$, and $C_0/(C_0 + C) \leq 25\%$, respectively (Cambardella et al. 1994).

Pearson correlation analysis was used to determine the relationships of the heavy-metal contents with terrain and slope hydrological factors. A one-way analysis of variance (ANOVA) was used to compare the difference between the mean heavy-metal contents in the types of sampling sites. The Mann-Kendall nonparametric test was used to evaluate the trend of heavy metal contents and concentrations in the soil and water along the river. The data were classically processed and analyzed using Excel 2013 and IBM SPSS 20, and the geostatistical analysis and interpolation were performed using GS+ 7.0 and ArcMap 10.1.

Results and discussion

Descriptive statistical characteristics of the heavy metals

The mean Pb, Zn, and Cd contents at the sampling types in the mining area (A–C) were 2028, 3794, and 14.8 mg kg^{-1}, with ranges of 1305–2995, 2861–5986, and 9.4–26.6 mg kg^{-1}, respectively, which were 8-, 19-, and 49-fold higher, respectively, than the second-level limits (250, 200, and 0.3 mg kg^{-1} for Pb, Zn, and Cd, respectively). The mean contents were also higher than the heavy metal contents in soils of other mining regions (Rodríguez et al. 2013; Krishna et al. 2013; Ding et al. 2017; Shen et al. 2017). The mean Pb, Zn, and Cd contents in the nearby farmland (site type D, Table 2), however, were 76.4, 130, and 0.18 mg kg^{-1}, respectively, all of which were under the second-level limits of the Environmental Quality Standard for Soils of China (1995). The means of the heavy metals differed significantly between the site types (Fig. 2; ANOVA, $p < 0.01$), except for Pb, where the mean contents in B and C did not differ significantly. Specifically, mean Pb, Zn, and Cd contents were highest in A and lowest in D, but $Zn(B) < Zn(C)$ and $Cd(B) > Cd(C)$ in site types B and C, which may indicate that Zn content at site C was mainly affected by surface-water scouring and sedimentation and that Cd content was mainly due to leaching. The differences of the heavy-metal contents between the types of sampling sites depended mainly on the nature of the soils. The soil in A was new mineral-waste soil and had not been washed or leached by rainwater and so had the highest heavy-metal contents. The soils in B and C were also mineral-waste soil but had been naturally eroded for 6 and 12 months, respectively. The soil in D was farmland soil that had not been directly disturbed by mining activities, so the heavy-metal contents were the lowest. The heavy-metal contents were weakly spatially variable in A, weakly to moderately variable in B and C, and moderately variable in D, mainly due to the distance between the samples. The distance was several meters for A, tens of meters for B and C, and several kilometers for D. Brocca et al. (2012) and Zhang et al. (2015) have reported that an increase in sampling range was an important reason for an increase in the variability of variables.
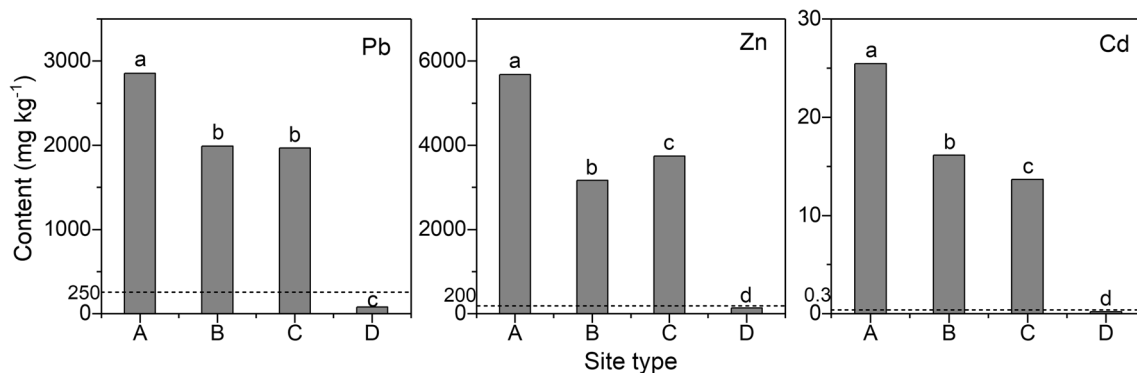
Fig. 2 Mean Pb, Zn, and Cd contents in site types A, B, C, and D. Different lowercase letters above the bars indicate significant difference among different site types

Spatial distribution of heavy metals

We analyzed the spatial distributions of Pb, Zn, and Cd in site types C and E. Type C had a wider experimental area than types A and B and a gentle slope. More importantly, C had a clear flow path, which provided conditions for analyzing the influence of surface hydrological processes on the distributions of heavy metals. For type E, we wanted to determine the trend of variation of the three heavy metals along the river by sampling and analyzing the samples of soil and water from the discharge point of treated runoff (E0) to the downstream 8 km.

Spatial distribution of heavy metals in site type C

The data for Pb, Zn, and Cd contents in site type C within the mining area were normally or approximately normally distributed. The kurtosis and skewness of Pb content were slightly > 1, and kurtosis and skewness for both Zn and Cd were < 1. A Q-Q plot and K-S analysis also indicated that the Pb, Zn, and Cd contents were normally or approximately normally distributed, which could thus be geostatistically analyzed without transforming the data (Yu et al. 2019; Zhu et al. 2019). Each of the heavy metals fit well and indicated apparent spatial structure of the geostatistical semivariograms (Fig. 3). The parameters of semivariance structure (Table 3) further indicated that Pb and Cd contents were strongly spatially dependent and that Zn content was moderately spatially dependent at the

small scale of the sloping mineral-waste soil in site type C, where all dependences and variabilities were spatially isotropic (anisotropic ratio < 2.5) (Trangmar et al. 1985). Pb, Zn, and Cd contents each had their own best fit semivariance models, which were spherical, linear, and exponential, respectively, and all coefficients of determination (R^2) were high, indicating good fits. The ranges for Pb, Zn, and Cd were 4.0, 9.9, and 4.7 m, respectively, all of which were larger than the sampling interval (2–4 m) in this study, indicating that an interval of 2×4 m was reasonable for sampling and analyzing the structure and dependence of the spatial variabilities of the heavy metals on the slope. Maps of the spatial distributions were interpolated using ordinary kriging based on the geostatistical parameters of Pb, Zn, and Cd (Fig. 4). Pb, Zn, and Cd contents had obvious patterns of spatial distribution on the gentle slope, with the contents generally decreasing from north to south. The gentle slope had developed from types A and B and had only eroded naturally after the original artificial disturbance. The influence of the terrain and hydrological slope factors on the distribution of Pb, Zn, and Cd should thus be analyzed further.

The relationships of the terrain factors elevation, slope, and aspect and the slope hydrological factors FD and FA with the three heavy-metal contents were analyzed using Pearson correlation (Table 4). The terrain and slope hydrological factors were not significantly correlated with the three heavy-metal contents, inconsistent with the results reported by Ding et al. (2017). This inconsistency may
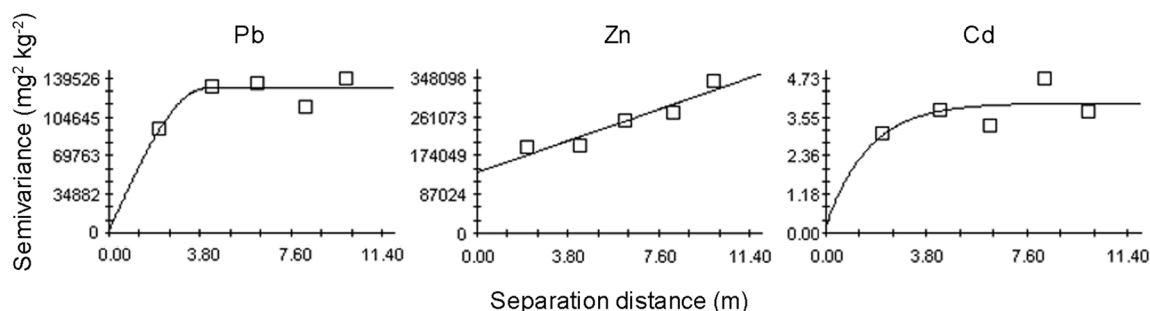

Fig. 3 Experimental semivariograms and the best fitted models for Pb, Zn, and Cd contents in site type C

Table 3 Geostatistical parameters of Pd, Zn, and Cd contents in site type C

Heavy metal	Model	Nugget (C_0)	Sill ($C + C_0$)	Range (m)	$C/(C + C_0)$ (%)	R^2	Anisotropic ratio
Pb	Spherical	1900	130,400	4.01	98.5	0.750	1.138
Zn	Linear	136,556	320,501	9.91	57.4	0.898	1.000
Cd	Exponential	0.170	3.984	4.74	95.7	0.381	1.951

have been due to the small scale (15 × 20 m) of this site type; the effects of the terrain and hydrological factors would be limited to some extent in the relatively small slope of the mineral-waste soil. We could nevertheless also generally determine the trends of the contents of the three heavy metals with the terrain and hydrological factors: Pb, Zn, and Cd contents tended to decrease as the slope, FD and FA increased (Fig. 5), which was mainly caused by washing by runoff and leaching by rainwater, consistent with the results reported by Lu et al. (2017) for another mining area. The correlations among the Pb, Zn, and Cd contents were significant with each other, indicating that the three heavy metals had the same anthropogenic source (Shen et al. 2017), i.e., mining activity.

Spatial distribution of heavy metals in site type E along the river

The descriptive statistical parameters of Pb, Zn, and Cd contents in the soil and water along the river from 2 km upstream to 8 km downstream from the discharge point (E0) are presented in Table 5. The mean Pb, Zn, and Cd contents in the soil were 147, 195, and 0.95 mg kg^{-1}, with ranges of 62.2–453, 77.6–480, and 0.04–3.66 mg kg^{-1},

respectively. Pb and Zn contents were moderately spatially variable, and Cd content was strongly spatially variable. All three mean contents were below the second-level limits of the environmental quality standard for soils of China, but the maximum values were 1.8-, 2.4-, and 12.2-fold higher than the limits for Pb, Zn, and Cd, respectively. The mean Pb, Zn, and Cd concentrations in the river water were 1.19, 109, and 0.35 μg L^{-1}, with ranges of 0.18–3.09, 15.3–185, and 0.03–1.16 μg L^{-1}, respectively. All three mean values and even the maximum values were below the second-level limits for surface water of China. All three heavy-metal concentrations were moderately spatially variable, in the order Zn < Pb < Cd, consistent with the variabilities in the riverside soil, indicating that the relative magnitudes of the variabilities of heavy metals were even generally similar in different carriers.

The distributions of the heavy metals in the riverside soil and the river water clearly varied from 2 km upstream to 8 km downstream from the discharge point ($x = 0$, Fig. 6). Soil Pb content first decreased and then increased but exceeded the second-level limit for soil only at the point 2 km upstream and generally tended to increase but not significantly (M-K test, $p > 0.05$). Zn and Cd contents slowly increased near the discharge point and exceeded the
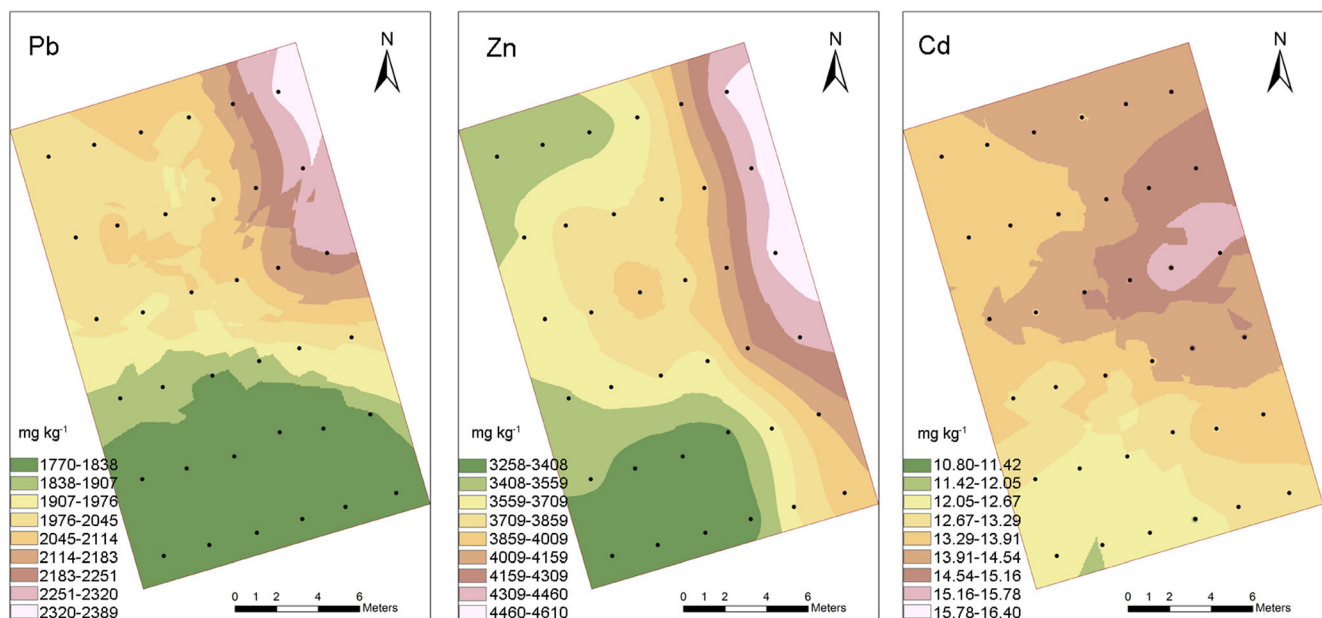

Fig. 4 Maps of the spatial distribution of Pd, Zn, and Cd contents (mg kg^{-1}) in site type C

Table 4 Pearson correlation coefficients between Pb, Zn, and Cd contents and the geographical and hydrological factors in site type C

	Elevation	Slope	Aspect	FD	FA	Pb	Zn	Cd
Elevation	1							
Slope	− 0.122	1						
Aspect	− 0.256	0.018	1					
FD[a]	0.164	− 0.164	0.149	1				
FA[b]	0.064	− 0.181	0.101	− 0.105	1			
Pb	0.318	− 0.122	− 0.058	− 0.064	− 0.083	1		
Zn	− 0.036	− 0.014	0.131	− 0.187	− 0.189	0.569[**c]	1	
Cd	0.056	− 0.167	− 0.015	− 0.060	− 0.189	0.455[**]	0.820[**]	1

[a] Flow direction

[b] Flow accumulation

[c] $p < 0.01$

second-level limits 5–8 km downstream, and both generally tended to significantly increase ($p < 0.01$), which was not expected. This abnormal increase may have been due to the stacking and discharge of domestic waste in the lower course of the river; heavy metals from the waste may have affected the spatial distributions and trends of variation of the heavy metals in the soil along the river (Yin et al. 2015; Kim et al. 2015). Pb, Zn, and Cd concentrations in the river water had similar trends, decreasing downstream from the discharge point due to the transport and diffusion of the metals by the river water, and the decreasing trends were significant at $p < 0.01$, 0.05, and 0.01, respectively. The decreasing trends of Pb, Zn, and Cd concentrations in the river water were consistent with the results reported by Ding et al. (2017).

Risk assessment of heavy metals

Four common indices, P, P_N, RI, and I_{geo}, were used to assess the degree of pollution and the potential environmental risk of the heavy metals for the soils in A–E (Table 6). All indices for the mining area (A–C) indicated in a high level of contamination. Each of the four indices was highest for the new mineral-waste soil in site type A. P and P_N indicated heavy contamination, RI was much higher than 600, indicating a very high potential ecological risk, and I_{geo} was > 5, also indicating a severe level of pollution. P, P_N, I_{geo}, and RI in B and C, where the mineral-waste soil had been stacked for 6 and 12 months, respectively, were also high and indicated heavy contamination and a high potential ecological risk. Most of the indices for outside the mining area (D and E) indicated a low level of
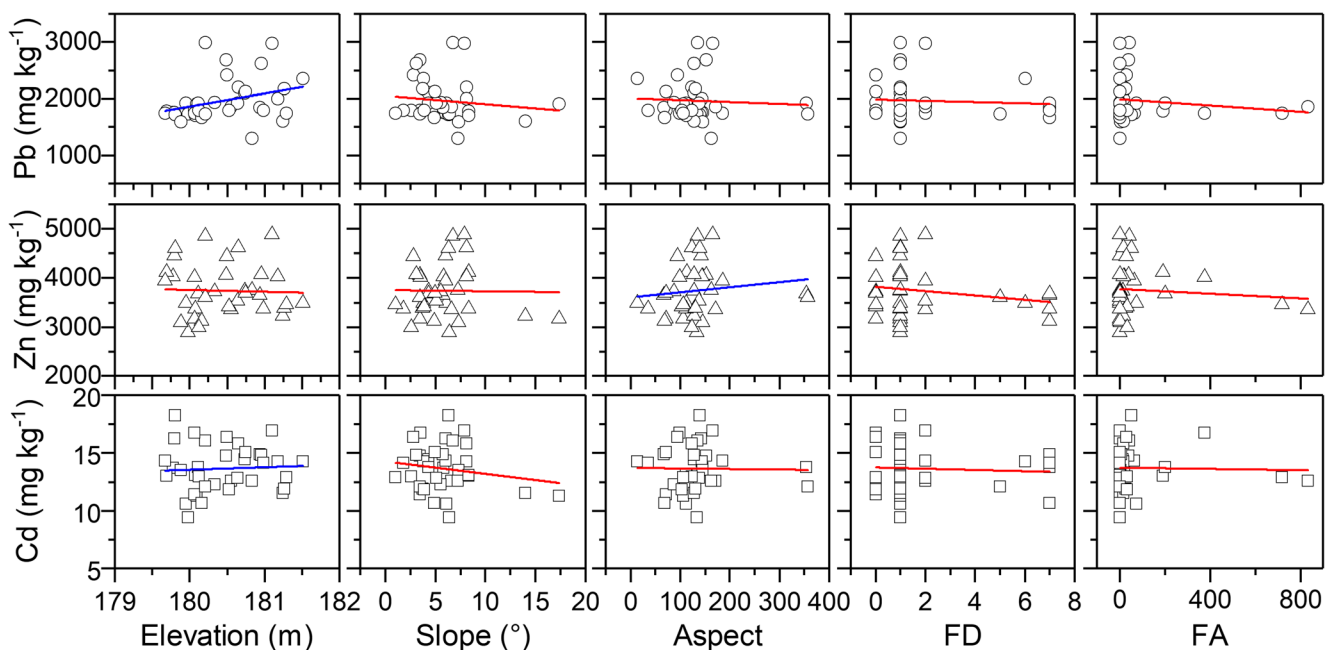

Fig. 5 Fitted curves for the geographical and hydrological factors and Pb, Zn, and Cd contents in site type C. Blue lines indicate an increasing trend, and red lines indicate a decreasing trend. FD, flow direction; FA, flow accumulation

Table 5 Descriptive statistics of Pb, Zn, and Cd contents (mg kg^{-1}) in the soil and concentrations (µg L^{-1}) in the river water in site type E

	Heavy metal	Minimum	Mean	Maximum	SD[a]	CV[b] (%)	Standard II[c]
Soil	Pb	62.2	147	453	108	73.2	250
	Zn	77.6	194	480	108	55.7	200
	Cd	0.04	0.95	3.66	1.03	109	0.3
Water	Pb	0.18	1.19	3.09	1.00	84.1	10
	Zn	15.3	109	185	53.0	48.5	1000
	Cd	0.03	0.35	1.16	0.32	90.7	5

[a] Standard deviation

[b] Coefficient of variation

[c] Second-level limit of the standard of environmental quality for soil (1995) and surface water (2002) in China

contamination. Both P and P_N were < 0.7 in D, indicating clean soil, RI was below the lowest level limit (150), indicating a low potential ecological risk, and I_{geo} was between 0 and 1 for the three heavy metals, indicating a low level of contamination. P_N at site type E was 2.5, indicating a moderate level of contamination, RI indicated a low potential ecological risk and I_{geo} indicated light to moderate contamination.

In summary, the soils in A, B, and C were heavily contaminated and had high potential ecological risks, the farmland soil in D was not or was lightly contaminated and had a low ecological risk, and the river bank soil in E was lightly or moderately contaminated and had a low ecological risk. These results indicated that the mineral-waste soil was heavily contaminated and had a high environmental risk but that the farmland and river had not yet been badly affected by the mining activity.

The runoff from the mineral-waste soil flows to the mountains and can enter people's lives by "sedimentation tank–groundwater–domestic water" in the long term. The runoff flows, however, flows down a grass-treated slope and then into a sewage-treatment plant and is then discharged into the river, forming a "runoff–river–farmland–food" chain of heavy-metal exposure. This analysis of environmental risk

indicated that the heavy metals in the mineral-waste soil far exceeded their limits and that the contents and concentrations in the farmland soil, river water, and bank soil were acceptable. These results indicated that the mining activity had not yet affected the surrounding environment, which may also have little influence on local production and life if the waste soil was appropriately treated.

Conclusions

We determined the contents of three typical heavy metals, Pb, Zn, and Cd, in five types of sampling sites within and outside a mining area and determined the spatial distributions of Pb, Zn and Cd on a typical slope of mineral-waste soil in the mining area and along a river channel adjacent to beside the mining area. The mean Pb, Zn, and Cd contents were 2856, 5686, and 25.4 mg kg^{-1} in the newly produced mineral-waste soil; 1989, 3162, and 16.1 mg kg^{-1} in the mineral-waste soil that had been stacked for 6 months and 1966, 3742, and 13.7 mg kg^{-1} in the mineral-waste soil that had been stacked for 12 months, respectively, and differed significantly between the site types. All contents far exceeded the second-level limits
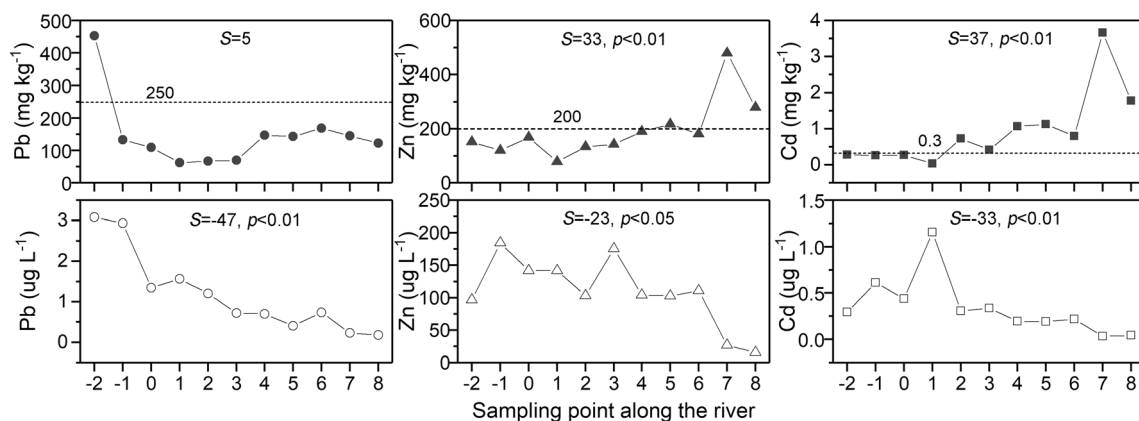

Fig. 6 Spatial distribution of Pb, Zn, and Cd contents in the soil (upper graphs) and concentrations in the river water (lower graphs) in site type E along the river. See Fig. 1a for the positions of the sampling points. Dotted lines in the upper graphs represent the second standard values. S is the Mann-Kendall test statistic, where $S > 0$ indicates an increasing trend and $S < 0$ indicates a decreasing trend, and p is the significance of the Mann-Kendal test statistic

Table 6 Assessment indices for Pb, Zn, and Cd sampled at site types A–D. P, single-factor pollution index; P_N, Nemerow synthetic pollution index; RI, potential ecological risk index; and I_{geo}, geoaccumulation index

Location	Site type	P			P_N	RI	I_{geo}		
		Pb	Zn	Cd			Pb	Zn	Cd
Inside the mining area	A	11.4	28.4	84.8	66.8	2630	5.9	5.8	7.3
	B	8.0	15.8	53.8	42.2	1669	5.4	4.9	6.6
	C	7.9	18.7	45.5	36.4	1423	5.3	5.2	6.4
Outside the mining area	D	0.31	0.65	0.61	0.59	20.5	0.66	0.33	0.18
	E	0.59	0.97	3.2	2.5	98.8	1.6	0.90	2.6

of the standards of environmental quality for soil in China and indicated heavy contamination and a very high ecological risk. The mean Pb, Zn, and Cd contents were 76.4, 131, and 0.18 mg kg^{-1} in the soil in the nearby farmland and 147, 195, 0.95 mg kg^{-1} in the soil along the river, most of which were below the second-level limits and indicated no or light contamination and low ecological risks. Pb, Zn, and Cd contents in the 12-month-old mineral-waste soil had apparent spatial structures and strong, strong and moderate spatial dependences, respectively. The contents generally decreased from north to south and were consistent with the flow direction and path of the slope. The contents of the three heavy metals tended to increase in the soil and decrease in the water along the river. This study found that the mineral-waste soil was heavily contaminated and posed a high ecological risk to the surrounding environment but it had not yet heavily polluted the surrounding farmland and river water. Appropriate measures should nevertheless be taken to reduce the effects of the mining activity.

References

Alary C, Demougeot-Renard H (2010) Factorial kriging analysis as a tool for explaining the complex spatial distribution of metals in sediments. Environ Sci Technol 44:593–599

Bednářová Z, Kalina J, Hájek O, Sáňka M, Komprdová K (2016) Spatial distribution and risk assessment of metals in agricultural soils. Geoderma 284:113–121

Brocca L, Tullo T, Melone F, Moramarco T, Morbidelli R (2012) Catchment scale soil moisture spatial–temporal variability. J Hydrol 422:63–75

Cambardella CA, Moorman TB, Novak JM, Parkin TB, Karlen DL, Turco RF, Konopka AE (1994) Field-scale variability of soil properties in Central Iowa soils. Soil Sci Soc Am J 58:1501–1511

Chen T, Liu XM, Li X, Zhao KL, Zhang JB, Xu JM, Shi JC, Dahlgren RA (2009) Heavy metal sources identification and sampling uncertainty analysis in a field-scale vegetable soil of Hangzhou, China. Environ Pollut 157:1003–1010

Ding Q, Cheng G, Wang Y, Zhuang DF (2017) Effects of natural factors on the spatial distribution of heavy metals in soils surrounding mining regions. Sci Total Environ 578:577–585

Duan XW, Zhang GL, Rong L, Fang HY, He DM, Feng DT (2015) Spatial distribution and environmental factors of catchment-scale soil heavy metal contamination in the dry-hot valley of upper Red River in southwestern China. Catena 135:59–69

Fu S, Wei CY (2013) Multivariate and spatial analysis of heavy metal sources and variations in a large old antimony mine, China. J Soils Sediments 13:106–116

Hakanson L (1980) An ecological risk index for aquatic pollution control.a sedimentological approach. Water Res 14:975–1001

Kim HK, Jang TI, Kim SM, Park SW (2015) Impact of domestic wastewater irrigation on heavy metal contamination in soil and vegetables. Environ Earth Sci 73:2377–2383

Krishna AK, Mohan KR, Murthy NN, Periasamy V, Bipinkumar G, Manohar K, Rao SS (2013) Assessment of heavy metal contamination in soils around chromite mining areas, Nuggihalli, Karnataka, India. Environ Earth Sci 70:699–708

Li YT, Becquer T, Dai J, Quantin C, Benedetti MF (2009) Ion activity and distribution of heavy metals in acid mine drainage polluted subtropical soils. Environ Pollut 157:1249–1257

Liang J, Feng CT, Zeng GM, Gao X, Zhong MZ, Li XD, Li X, He XY, Fang YL (2017) Spatial distribution and source identification of heavy metals in surface soils in a typical coal mine city, Lianyuan, China. Environ Pollut 225:681–690

Liu BL, Ma XW, Ai SW, Zhu SY, Zhang WY, Zhang YM (2016) Spatial distribution and source identification of heavy metals in soils under different land uses in a sewage irrigation region, Northwest China. J Soils Sediments 16:1547–1556

Lu HZ, Cao LX, Liang Y, Yuan JQ, Zhu YY, Wang Y, Gu YL, Zhao QG (2017) Mineral-leaching chemical transport with runoff and sediment from severely eroded rare-earth tailings in southern China. Solid Earth 8:845–855

Ma L, Yang ZG, Li L, Wang L (2016) Source identification and risk assessment of heavy metal contaminations in urban soils of Changsha, a mine-impacted city in southern China. Environ Sci Pollut Res 23:17058–17066

Maas S, Scheifler R, Benslama M, Crini N, Lucot E, Brahmia Z, Benyacoub S, Giraudoux P (2010) Spatial distribution of heavy metal concentrations in urban, suburban and agricultural soils in a Mediterranean city of Algeria. Environ Pollut 158:2294–2301

Marrugo-Negrete J, Pinedo-Hernández J, Díez S (2017) Assessment of heavy metal pollution, spatial distribution and origin in agricultural soils along the Sinu River basin, Colombia. Environ Res 154:380–388

National environmental monitoring Centre of China (1990) Background values of soil elements of China. China Environmental Science Press, Beijing

Nielsen DR, Bouma J (1985) Soil spatial variability. Pudoc, Wageningen

Reza SK, Baruah U, Singh SK, Das TH (2015) Geostatistical and multivariate analysis of soil heavy metal contamination near coal mining area, northeastern India. Environ Earth Sci 73:5425–5433

Rodrigues S, Pereira ME, Sarabando L, Lopes L, Cachada A, Duarte A (2006) Spatial distribution of total hg in urban soils from an Atlantic coastal city (Aveiro, Portugal). Sci Total Environ 368:40–46

Rodríguez L, Ruiz E, Alonso-Azcárate RJ (2013) Heavy metal distribution and chemical speciation in tailings and soils around a Pb-Zn mine in Spain. J Environ Manag 90:1106–1116

Shen F, Liao RM, Ali A, Mahar A, Guo D, Li RH, Sun XN, Awasthi MK, Wang Q, Zhang ZQ (2017) Spatial distribution and risk assessment of heavy metals in soil near a Pb/Zn smelter in Feng County, China. Ecotoxicol Environ Saf 139:254–262

Trangmar BB, Yost RS, Uehara G (1985) Application of geostatistics to spatial studies of soil properties. Adv Agron 38:45–94

Wang C, Liu SL, Zhao QH, Deng L, Dong SK (2012) Spatial variation and contamination assessment of heavy metals in sediments in the Manwan reservoir, Lancang River. Ecotoxicol Environ Saf 82:32–39

Wang LF, Yang LY, Kong LH, Li S, Zhu JR, Wang YQ (2014) Spatial distribution, source identification and pollution assessment of metal content in the surface sediments of Nansi Lake, China. J Geochem Explor 140:87–95

Wang YQ, Yang LY, Kong LH, Liu EF, Wang LF, Zhu JR (2015) Spatial distribution, ecological risk assessment and source identification for heavy metals in surface sediments from Dongping Lake, Shandong, East China. Catena 125:200–205

Yan WB, Mahmood Q, Peng DL, Fu WJ, Chen T, Wang Y, Song L, Chen JR, Liu D (2015) The spatial distribution pattern of heavy metals and risk assessment of moso bamboo forest soil around lead-zinc mine in southeastern China. Soil Tillage Res 153:120–130

Yin YC, Wang LL, Xiao L, Li YW, Peng H, Qi H, Deng SH (2015) Characteristics and sources of heavy metal pollution in urban sub-urban and rural domestic waste of Chengdu, China. Chin J Environ Eng 9:392–400

Yu DX, Jia XX, Huang LM, Shao MA, Wang J (2019) Spatial variaiton of soil bulk density in different soil layers in the loess area and simulation. Acta Pedol Sin 56:55–64

Zhang PP, Shao MA, Zhang XC (2015) Scale-dependence of temporal stability of surface-soil moisture in a desert area in northwestern China. J Hydrol 527:1034–1044

Zhu XC, Shao MA, Liang Y, Tian ZY, Wang X, Qu LL (2019) Mesoscale spatial variability of soil-water content in an alpine meadow on the northern Tibetan plateau. Hydrol Process:33 https://doi.org/10.1002/hyp.13479